

RESEARCH

Open Access



Comparative Thermal Evaluation of Two Systems of Wall Panels Exposed to Hot and Arid Arabian Environmental Weather Conditions

Luai Mohammed Alhems¹, Aftab Ahmad¹, Mohammed Ibrahim¹, Mohammed Rizwan Ali^{1*}  and Madyan A. Al-Shugaa²

Abstract

Thermal evaluation of twin wall panel systems was assessed under vibrant hot and arid conditions of weather in the Arabian Peninsula. Two systems of wall panels (0.6 m × 0.6 m) were prepared. The first system was prepared with a 5.0 cm thick extruded polystyrene (XPS) board. While the second system was prepared with 5.0 cm thick layer of foam-mortar encompassing expanded polystyrene (EPS) beads. Both the thermal insulative layers were sandwiched between two 7.5 cm thick concrete layers. The two wall panel systems were thermally evaluated at the same time in a carefully designed test room. Comparison was accomplished between the two wall systems by measuring the U -value (thermal transmittance) and R -value (resistance). The U -value (air to air) for sandwiched XPS concrete wall system was $0.837 \text{ W/m}^2 \text{ K}$ while it was $2.527 \text{ W/m}^2 \text{ K}$ for sandwiched EPS beads foam-mortar concrete wall system. The mean U -values (surface to surface) of the sandwiched XPS concrete wall system was $1.143 \text{ m}^2 \text{ K/W}$ and $0.293 \text{ m}^2 \text{ K/W}$ for sandwiched EPS beads foam-mortar concrete wall system. The sandwiched XPS concrete wall system was more efficient than the sandwiched EPS beads foam-mortar concrete wall system in terms of thermal performance. About 4.5 h of time lag was observed for both the wall panel systems between the external surface temperature and the heat transmission in the internal surface. The output of the FEM simulation by ABAQUS is compared with the measured data for Set-1 (period 16-Aug-2022 to 26-Aug-2022). The hourly temperature change on the outer and inner surfaces has good agreement for both sandwiched XPS concrete wall system and sandwiched EPS beads foam-mortar concrete wall system. The simulation can also predict the heat flux through the two wall systems investigated.

Practical application

This research was carried out with a view to explore the possibility of using thermally insulating materials for buildings. The outcomes showed that the system proposed has performed well in the Arabian Gulf environment which can be easily adopted in the field.

Keywords Thermal performance, Thermal transmittance, Thermal resistance, Wall panel, Heat flow rate

Journal information: ISSN 1976-0485 / eISSN 2234-1315.

*Correspondence:

Mohammed Rizwan Ali
rizwanm@kfupm.edu.sa

Full list of author information is available at the end of the article



© The Author(s) 2024. **Open Access** This article is licensed under a Creative Commons Attribution 4.0 International License, which permits use, sharing, adaptation, distribution and reproduction in any medium or format, as long as you give appropriate credit to the original author(s) and the source, provide a link to the Creative Commons licence, and indicate if changes were made. The images or other third party material in this article are included in the article's Creative Commons licence, unless indicated otherwise in a credit line to the material. If material is not included in the article's Creative Commons licence and your intended use is not permitted by statutory regulation or exceeds the permitted use, you will need to obtain permission directly from the copyright holder. To view a copy of this licence, visit <http://creativecommons.org/licenses/by/4.0/>.

1 Introduction

As stringent conditions are being enforced by the international society for the sake of reducing the emissions of the greenhouse gases, research on building materials is currently focused to reduce energy consumption by developing thermally efficient building materials and systems. With the increasing cost of energy globally, conservation of energy is a priority in the developing world. The key to conserving energy of building systems is to select materials which are energy efficient and cost effective. According to the estimates about 77.7% of the electrical energy produced is being consumed by buildings to power them. While in desert regions air-conditioning consumes about 73% of the total energy needed by the buildings (Elhadidy et al., 2001; Annual Report, 2016). It is also a well-known fact that the energy requirements all over the globe are expected to rise firmly in the near future, development of energy proficient systems and materials for construction is the need of the hour. The external walls and windows, through which heat is transmitted, are the key components of the building envelope which determine energy efficiency. Thus, the development of energy efficient external walls and windows is essential for energy conservation. Furthermore, as building structures are heterogeneous in nature and poor workmanship can introduce thermal bridges, in such cases building structures can only be assessed through in situ measurements (Li et al., 2015; Wit et al., 2004; Bidulph et al., 2014; Luo et al., 2011).

R -value of a building component is an important parameter which determines the efficiency of a system. Several methods have been used to compute the system's R -value (Courville & Beck, 1989; Desogus et al., 2011). Finite volume scheme and Fourier analysis methods have been employed to compute the thermal capacitance and conductivity of a building envelope using temperature and heat flux sensors (Luo et al., 2010). Desogus et al. (2011) have used a test chamber for computation of a building's R -values using different methods. Results showed that the R -values obtained by both methods were in conformance with the basic measurement principles. Courville and Beck (Courville & Beck, 1989) have determined the in situ R -value of an insulation used in sloped roofs using four different techniques by the measurement of temperature variation and heat flow rate. Similar results were obtained by all four methods using computer code PROPOR. Computing of onsite R -value of a building component can be influenced by low-frequency temperature values. Convergence criteria were introduced by Flanders (1985) to counter the effect to determine the thermal resistance of an insulating material. Temperature and heat flux of the internal and external surfaces of the wall panels were measured by Sassine (2016) A new

methodology requiring minimum monitoring period was proposed. A thermal calculation was proposed to determine the equivalent thermal properties. A statistical model using lumped thermal mass was proposed by Gori et al. (2017) to estimate the transfer of heat in the building system. An optimization technique was proposed based on Bayesian to determine model parameters. This technique uses very minimal information about the building systems and materials used in construction.

Cabeza et al. (2010). extensively investigated the use of different insulating materials such as mineral wool, polystyrene and polyurethane. The experimental and theoretical in situ thermal transmittance values had a good convergence with difference as low as 12%. Peng and Wu (2008) calculated the onsite R -value of materials used in construction by measuring the internal and the external surface temperature of the building. Also the performance of a range of insulation materials has been studied over the years (Abdelrahman et al., 1993; Al-Aijlan, 2006; Al-Hammad et al., 2005; Budaiwi et al., 2002). The thermal resistance of the most widely used bricks has been determined using a guarded hot plate (Ahmad and Hadhrami, 2009; Al-Hadhrami and Ahmad, 2009). The thermal properties of a hollow block made of shale and having 29 rows of perforations has also been evaluated using a guarded heat box. The theoretical transfer coefficient of heat ($0.546 \text{ W/m}^2 \text{ K}$) was less than the investigated value determined by the guarded heat box ($0.726 \text{ W/m}^2 \text{ K}$) (Guo-liang et al., 2017). The shortcoming of this method is that it cannot be used for large samples such as, large walls or panels. Ahmad et al. (2014) have determined the onsite U -value and R -value of building's walls. They found that the U -value is related to the weather conditions and the wall orientation.

In the assessment of thermal insulating properties of a building envelop it is paramount to assess the effect of thermal bridges. Giorgio et al. (2018) studied the quantitative thermal bridges effect of three types of them by infrared thermography of different wall systems. According to the results of that study, the methodology adopted has shown that the hidden thermal bridges were quite visible which allowed them to accurately locate and rectify them.

Bagasi and Calautit (2020) conducted a study at the old traditional (Baeshen) family House in historic Jeddah which yielded several significant findings that could form future architectural design practices in similar regions. The study demonstrated that the closed Mashrabiya (perforated wall) panes contributed in reducing the flow of hot air into the rooms during afternoon and thus maintaining indoor temperatures in the range of $35.4 \text{ }^\circ\text{C}$ to $35.8 \text{ }^\circ\text{C}$. The most effective strategy was the use of wetted cloth near the Mashrabiya inlet which resulted

in indoor average temperature of 33.8 °C while the outdoor temperature was 41.6 °C. Their study also revealed that Mashrabiya with evaporative cooling alone was not able to provide comfort during mid-day in hot summer conditions. Their study indicated future work should be focused on investigating different materials and strategies to enhance the performance of Mashrabiya.

The study conducted by Aldossary et al. (2014) evaluated the domestic energy consumption patterns in a hot and arid climate of Riyadh city in Saudi Arabia. Their study utilized a multiple-case study approach to analyze energy usage in residential buildings considering the region's high energy consumption and carbon emission rates. Key aspects such as assessing energy consumption, identifying design weaknesses, and proposing energy retrofitting solutions to improve sustainability in residential buildings in Riyadh were discussed.

Kanagaraj et al.'s (2023) study explores the impact of nano composite materials on the impact strength of concrete at elevated temperatures in the range of 250 °C to 1000 °C. The author findings highlighted that the impact strength of concrete is directly influenced by factors such as the type and proportion of binder, heating intensity, duration, and cooling method. The study specifically noted the exceptional performance of the mix containing nano-cement when exposed to 1000 °C. Moreover, the investigation unveiled that the addition of nanomaterials contributed to increased compressive strength, densification of the internal structure, and enhanced impact resistance of concrete. Despite improving mechanical properties at room temperature, the study observed a decline in impact strength as temperatures rose, with the extent of loss influenced by the type and proportion of nanomaterials.

In the investigation conducted by Iqbal et al. (2022), three commonly accessible insulation materials such as glass wool, extruded polystyrene, and polyethylene were systematically assessed in a case study involving residential structures situated in a cold region of Pakistan. Thermal data were gathered over a 21-day period in 2019 using a Testo Saveries System and were subsequently analyzed to assess the thermal efficiency of each insulation material. The findings indicated that polyethylene emerged as the most cost-effective insulation material with superior thermal performance as compared to others. The author recommended the use of polyethylene in buildings located in cold regions of Pakistan.

Kangaraj et al. (2022) investigated the response of EPS wall panels with encapsulated concrete subjected to axial compression. Their findings revealed a transition in failure mode from brittle to ductile due to the encapsulation of concrete within the EPS system. The elastic characteristics of EPS played a crucial role in maintaining the

encapsulated concrete within the core even after failure. The presence of the EPS outer shell resulted in the wall panels exhibiting greater deformations compared to conventional brick masonry walls.

Prefabricated external thermal insulation composite systems are being extensively used for the sake of improving the thermal performance of existing buildings. In such an endeavor Roberto et al. (2017) investigated the on-site thermal performance of these systems and found that after installing them the thermal resistance of building envelopes has improved. However, floor slabs and anchors were identified as the most potential thermal bridges which were reducing the thermal efficiency of the whole building system.

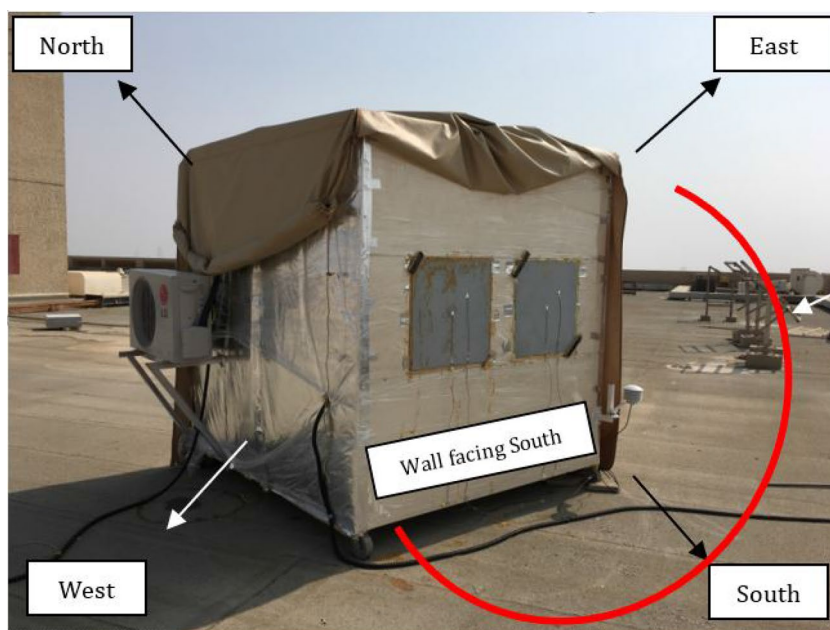
Thermal properties of building systems have been often assessed by analytical techniques. However, the actual thermal performances parameters of building envelope on-site often differ with the theoretical evaluation. To assess the differences between on-site and theoretical evaluation, Francesco et al. (2014) calculated these parameters and also estimated by conducting on-site measurements. They concluded that theoretically computed values were not in good agreement with the practical ones.

In the present work, measurements were conducted in a specially designed cubical test room to determine the U -value and R -value of small concrete wall panels under dynamic weather conditions. The thermal performance parameters were determined according to standard practices prescribed in the guidelines of international standards.

2 Experimental Set-Up

The thermal performance of two types of wall panel samples was determined under dynamic weather conditions. Two systems of wall panels (0.6 m×0.6 m) were prepared. The first system was prepared with a 5.0 cm thick extruded polystyrene (XPS) board. While the second system was prepared with 5.0 cm thick layer of foam-mortar encompassing expanded polystyrene (EPS) beads. Both the thermal insulative layers were sandwiched between two 7.5 cm thick concrete layers. These two panel systems were tested simultaneously for the evaluation of their thermal performance in a specially designed air-conditioned test room shown in Fig. 1.

The test room was a 2 m×2 m×2 m cubic room with two 0.6 m×0.6 m openings on the south facing wall for the installation of the test samples. The test room was completely insulated. The internal view of the test room as shown in Fig. 2, displays the two test samples with thermocouples and heat flux sensors mounted at locations 1 and 2, respectively, for both samples. A view



Arch showing the daylight exposure on the experimental room

Fig. 1 Test room established for the experiment

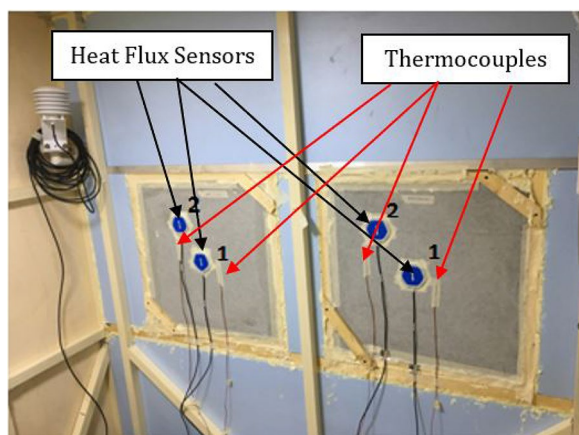


Fig. 2 View of the test room from inside with two systems of wall panels mounted (left: sandwiched XPS concrete wall system panel; right: sandwiched EPS foam-mortar concrete wall system panel)

through the section of the two test samples is shown in Fig. 3.

The two types of wall systems namely sandwiched XPS concrete wall system and sandwiched EPS beads foam-mortar concrete wall system were installed in the openings on the south wall of the test room. The samples and test room were equipped with sensors such as thermocouples, heat flow transducer, and air temperature transducer. Two sensors for measuring heat flux were mounted on the internal surface of each wall panel system and thermocouples were connected to both internal

and external surfaces. Also, air temperature transducers were fixed on the internal and external surfaces of the of the test room to measure the air temperature. A one-ton split type air-conditioning system was installed to control the room air temperature which was set at 19 °C throughout the test period.

The instrumentation used for the evaluation of the thermal performance of the two types of wall panel samples is shown in Table 1 and all the heat and temperature sensors were connected to a data logger.

Data were acquired at one-minute interval and the half-hourly averaged data was stored in the data logger memory during the entire test period. The collected data were downloaded from the memory of the data logger for further processing.

2.1 Test Method

Typically, onsite thermal parameters are determined by the thermal resistance (R -value) and the thermal transmittance (U -value) of building components. In this study, international standard methods described in ASTM C1155 (ASTM Co 1155, 2021a)/C1046 (ASTM Co 1046, 2021b) and ISO 9869 (ISO 9869, 1994) standards were used to evaluate these parameters. Sensors for measuring heat flux were positioned on the internal surface of the wall panel sample according to the recommendations of ASTM C1060 (ASTM Co 1060, 2015). Fig. 4 depicts the infrared images of the internal surface of the two types of wall panels which were captured by the infrared camera.

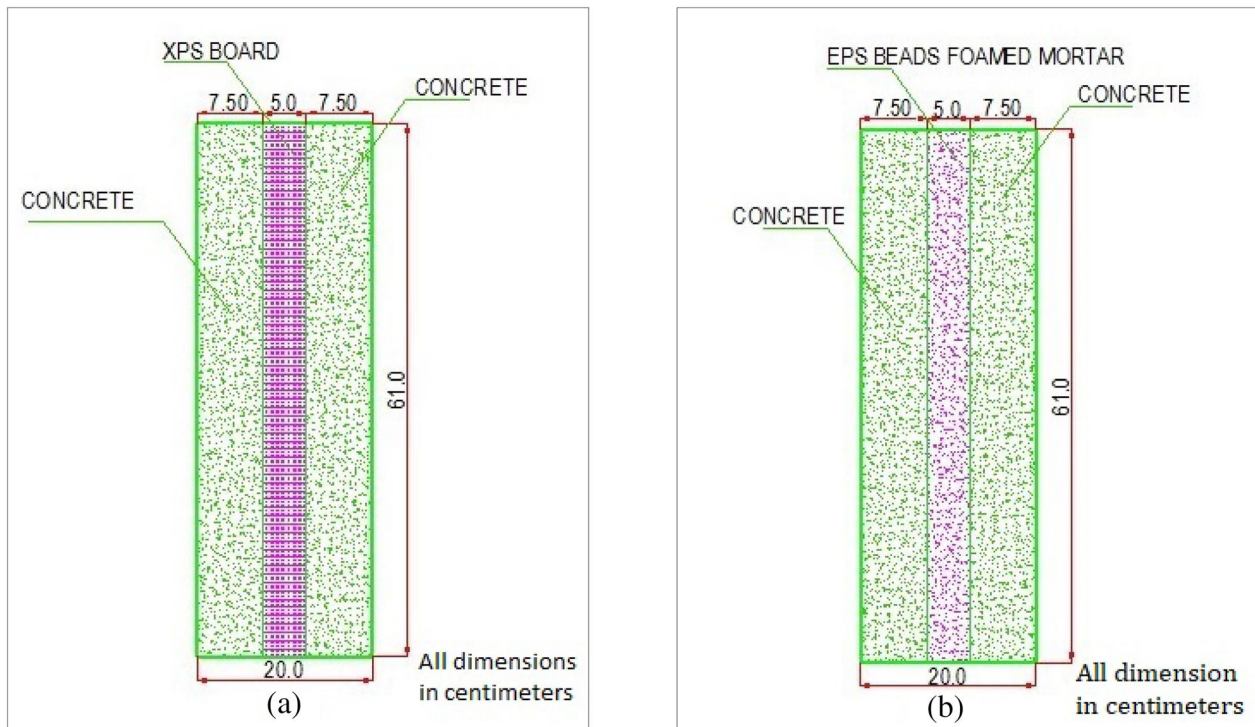


Fig. 3 View of the section of the of the two types of tested wall panel systems. **a** Sandwiched XPS concrete wall panel. **b** Sandwiched EPS beads foam-mortar concrete wall panel

Table 1 Instrumentation used in the experiment

Parameter/data logger	Type/manufacturer	Range	Accuracy
Temperature of the external surface of the wall panel sample	Type T Thermocouple, Omega Engineering Inc., USA	0 to 350 °C	±0.5 °C
Temperature of the internal surface of the wall panel sample	Type T Thermocouple, Omega Engineering Inc., USA	0 to 350 °C	±0.5 °C
Air temperature inside the test room	T108, Campbell Scientific Inc., USA	− 5 to 95 °C	±0.5 °C
External air temperature	T108, Campbell Scientific Inc., USA	− 5 to 95 °C	±0.5 °C
Heat flux	HFP01, Hukseflux	±2000 W/m ²	±5%
Thermal image	E8, FLIR Systems Thermal Imaging Infrared Camera	320 × 240 IR resolution	±2.0 °C
Data logger	CR1000, Campbell Scientific Inc., USA	Input ± 5000 mV	±0.06% of reading

The parameters measured included the internal and external surface temperature, internal and external air temperature, and the heat flow rate through the wall system panels. Internal and external surface temperature of both wall samples were measured at two locations. Heat flux sensors were also installed at two distinct locations on the internal surface of both test samples. The heat flow rate and the surface and air temperatures of the two test wall system panels were recorded simultaneously by the data logger.

The *R*-value is calculated by the concurrent recording of the time average heat flow rate and the difference in surface temperature of the wall panel samples, while the *U*-value is calculated by the concurrent recording of the difference in air temperature and time averaged heat flow rate.

2.2 Computation of the Thermal Parameters

The *R*-value (surface to surface) and the *U*-value (air to air) of the two wall panel samples were calculated

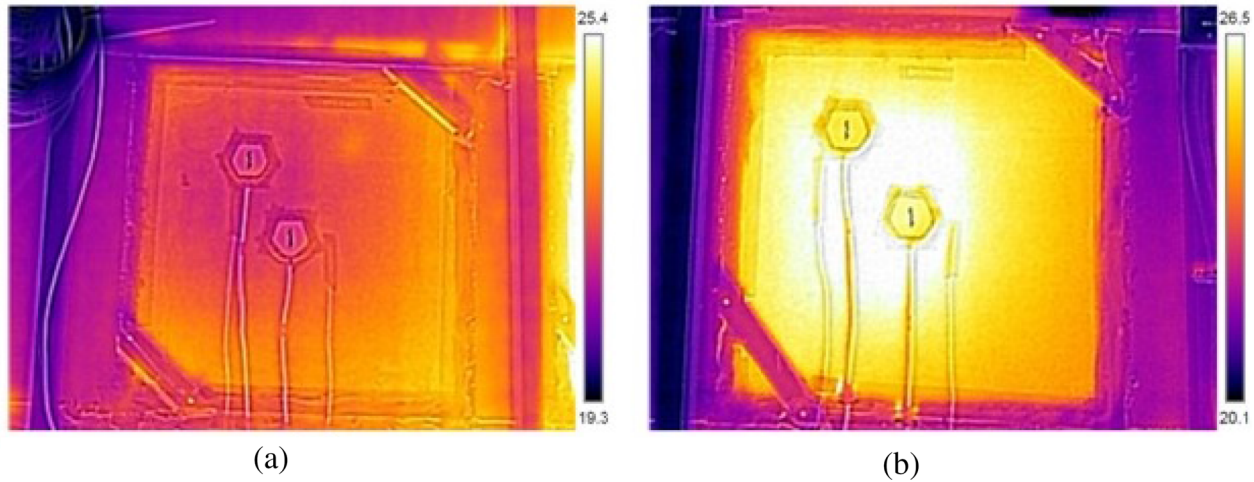


Fig. 4 Images by infrared thermograph camera of the tested wall panel systems. **a** Sandwiched XPS concrete wall panel. **b** Sandwiched EPS beads foam-mortar concrete wall panel

according to the average method described in international standards such as ISO 9869 (ISO 9869, 2014) and ASTM C1155 (ASTM Co1155, 2021a, 2021b).

The R -value was obtained utilizing Eq. (1).

$$R = \frac{\sum_{j=1}^m (T_{sej} - T_{sij})}{\sum_{j=1}^m q_j} \tag{1}$$

This equation calculates the R -value using temperatures (T_{sej} and T_{sij}) and heat flow rates (q_j).

The U -value was calculated utilizing Eq. (2).

$$U = \frac{\sum_{j=1}^m q_j}{\sum_{j=1}^m (T_{ej} - T_{ij})} \tag{2}$$

This equation calculates the U -value involving temperatures (T_{ej} and T_{ij}) and heat flow rates (q_j).

The method described in ASTM Co 1155-95 (ASTM Co 1155, 2021a, 2021b) was used to obtain the convergence factor and is given by Eq. (3).

$$CR_n = \frac{R(t) - R(t - n)}{R(t)} \times 100. \tag{3}$$

This equation computes the convergence factor using the R -values at different time steps ($R(t)$, $R(t - n)$), where: m is the total number of time steps, T_{sej} and T_{sij} are temperatures related to the sample surface, T_{ej} and T_{ij} are temperatures related to the ambient environment, q_j represents heat flow rates, CR_n is the convergence factor at time t .

The thermal conductance (C) is the inverse of the thermal resistance, i.e., $C = 1/R$, and the total thermal resistance (air to air) is the inverse of the thermal transmittance, i.e., $R_T = 1/U$. The total thermal resistance includes the resistance of the external and internal surfaces.

3 Measured Data Analysis

The thermal efficiency of the two different types of wall panel systems was assessed simultaneously under changing weather conditions during the summer of 2022 (i.e., from 16 August, 2022 to 28 September, 2022). To compute the thermal parameters of the test samples, 3 sets of experimental data were obtained and statistically examined.

The local weather conditions, such as the wind speed and the solar intensity affect the thermal transmittance of a building envelope as demonstrated by Ahmad et al. (2014). The atmospheric data were obtained from the locally installed weather station. The wind speed frequency distribution diagram for the test location for the period of testing is presented in Fig. 5. The data indicate that the prevailing wind direction (WD) at the test location during the measurement period was East of North-East (ENE). The maximum intensity of the horizontal global solar irradiance recorded during the measurement period at the test location is 984 W/m^2 .

The measured experimental data for the sandwiched XPS concrete panel and sandwiched EPS beads foam-mortar concrete wall systems were analyzed and are presented in the following sections:

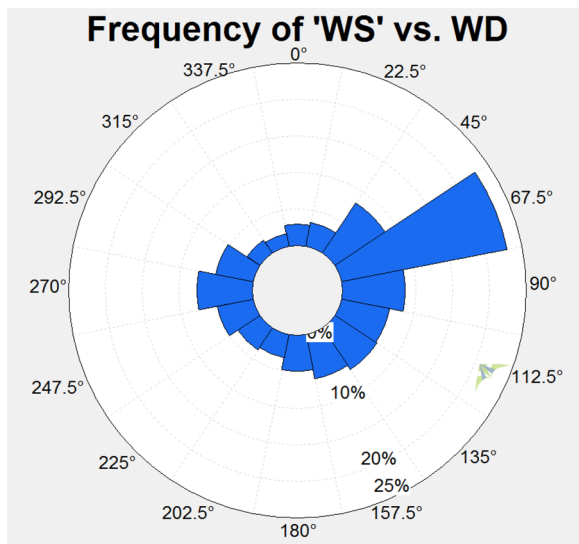


Fig. 5 Frequency distribution of the wind speed (WS) at the test location

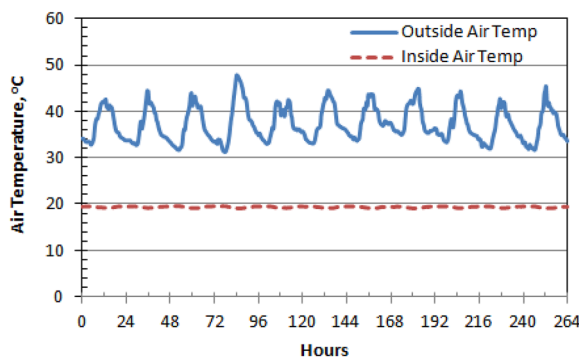


Fig. 6 Variation in the internal and external air temperature in the test room during the period of 16 August, 2022 to 26 August, 2022

3.1 Experimental Data Set-1: Testing Period—16 August, 2022 to 26 August, 2022

The experimental data set-1 was collected for a duration of 11 days starting from 16 August, 2022 to 26 August, 2022 for the two test wall samples. The thermal performance of both samples was assessed simultaneously. During the assessment both samples were exposed to the same internal air temperature and the same external air temperature in the test room. The air temperature measured for external and internal walls of the test set-up room is shown in Fig. 6. The internal air temperature is almost constant at about 19.3 °C while the external air temperature fluctuated during the monitoring period from 31.2 °C to 47.5 °C with an average value of 37.2 °C. Extremely hot weather conditions prevailed at the test location, and the minimum difference of air temperature

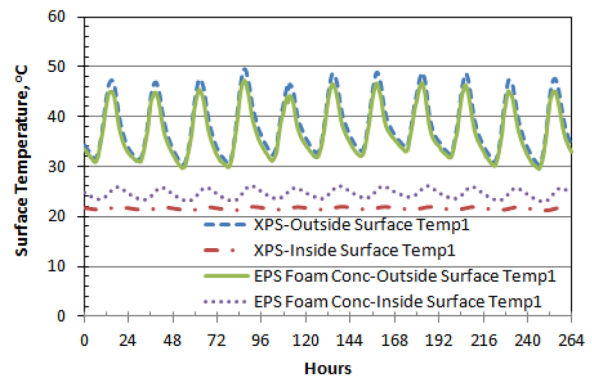


Fig. 7 Variation in the temperature of the internal and external surfaces of the two test systems during the period of 16 August, 2022 to 26 August, 2022

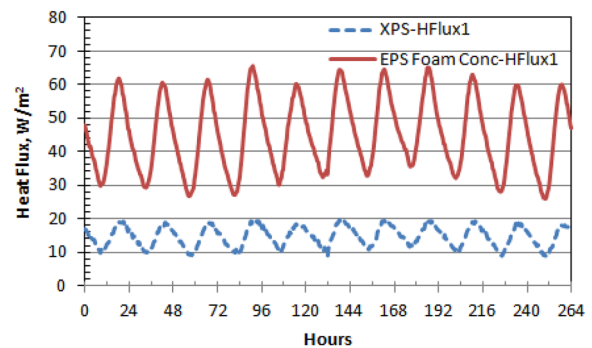


Fig. 8 Heat flow rate variation through the two test systems during the period of 16 August, 2022 to 26 August, 2022

recorded between the internal and external of the test room is 11.9 °C.

The temperature of the internal and external surfaces for the sandwiched XPS concrete wall system (XPS-External Surface Temp1) and sandwiched EPS foam-mortar concrete wall system (EPS Foam Conc-External Surface Temp1) wall panels are given in Fig. 7. The variation in the heat flux for the two test samples (XPS-HFlux1 and EPS Foam Conc-HFlux1) is shown in Fig. 8.

The data in Fig. 7 depicts that the change in temperature is cyclic for both internal and external surfaces of the test samples, with a lower temperature amplitude on the internal surface of both samples. The external surface temperature of the sandwiched XPS concrete wall system is higher than that of the sandwiched EPS foam-mortar concrete wall system. However, the trend is reversed for the internal surface. Variation of the heat flow rate of the two panels is depicted in Fig. 8. The heat flow rate variation is also cyclic for both test samples, with an average value of 14.7 W/m² for sandwiched XPS concrete wall system and 45.2 W/m² for sandwiched EPS foam-mortar concrete wall system. The results also indicate

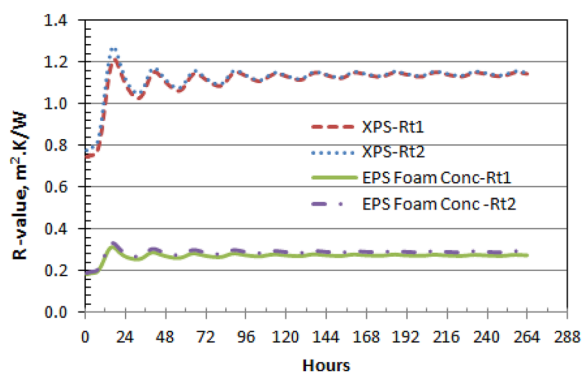


Fig. 9 R-value plot of the two test systems for data set 1

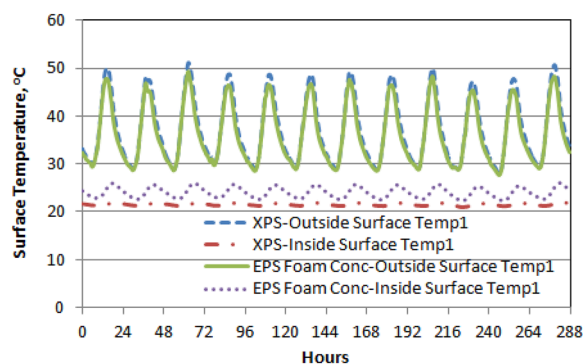


Fig. 11 Variation in the temperature of the internal and external surfaces of the two test systems during the period of 01 September, 2022 to 12 September, 2022

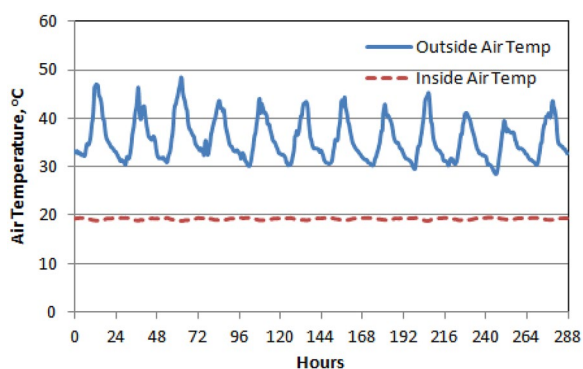


Fig. 10 Variation in the internal and external air temperature in the test room during the period of 01 September, 2022 to 12 September, 2022

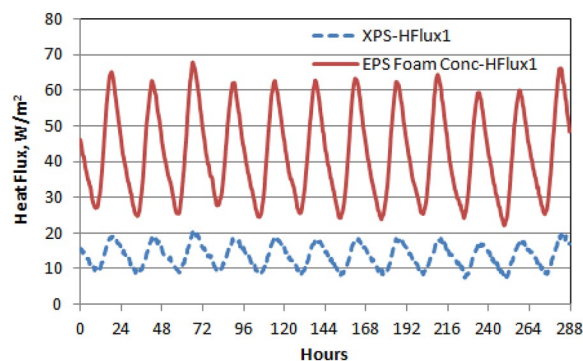


Fig. 12 Heat flow rate variation through the two test systems during the period of 01 September, to 12 September, 2022

that the average heat flux through the sandwiched EPS foam-mortar concrete wall system is about three times that through the sandwiched XPS concrete wall system sample. Variation of the running average of the R -value is presented in Fig. 9 which depicts that it approaches to a fixed value.

3.2 Experimental Data Set-2: Testing Period—01 September, 2022 to 12 September, 2022

The experimental data set-2 was collected during 12 days from 01 September, 2022 to 12 September, 2022 at the same location of the two test samples used to obtain data set-1. The air temperature measured on external and internal walls of the test set-up room is plotted in Fig. 10. The average internal air temperature is almost constant at about 19.3 °C, same as that recorded during the acquisition of data set-1, and the exterior air temperature fluctuated during the monitoring period from 28.6 °C to 48.4 °C, with an average value of 35.7 °C. The average exterior air temperature calculated using data set 2 is about 1.5 °C lower than that calculated using data set-1. However, the average

exterior air temperature is above 35 °C, and also the maximum temperature recorded during the acquisition of data set-2 is higher than that recorded during the acquisition of data set-1. The minimum difference of air temperature between the internal and exterior of the test room is 9.3 °C. Variation of the temperature of the internal and external surfaces of the two test samples is plotted in Fig. 11. Variation of the heat flux, calculated using data set-2, is shown in Fig. 12.

The data in Fig. 11 depicts that the change in temperature at both internal and exterior surfaces of the test samples is cyclic in nature, with the amount of temperature variation lower on the internal surface of both samples. The trends of temperature variation in data set-2 are similar to those observed in data set-1. Variation of the heat flux of the two wall panels is shown in Fig. 12. Variation of the heat flow rate is also cyclic for both test samples, with an average value of 13.7 W/m² for the sandwiched XPS concrete wall system sample and 42.4 W/m² for the sandwiched EPS foam-mortar concrete wall system sample. The average heat flux

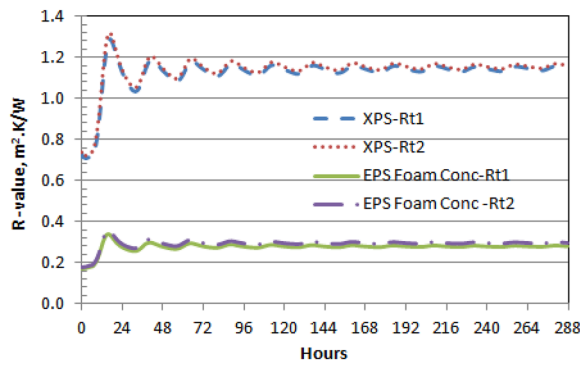


Fig. 13 *R*-value plot of the two test systems for data set 2

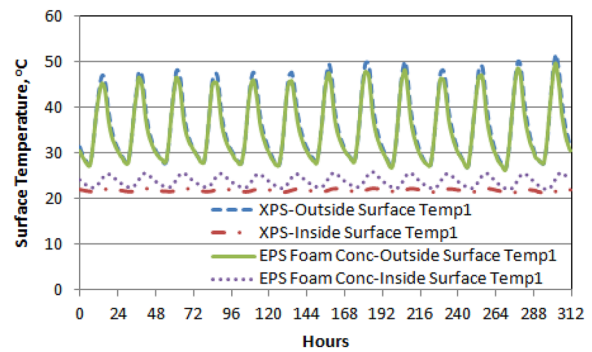


Fig. 15 Variation in the temperature of the internal and external surfaces of the two test systems during the period of 15 September, 2022 to 27 September, 2022

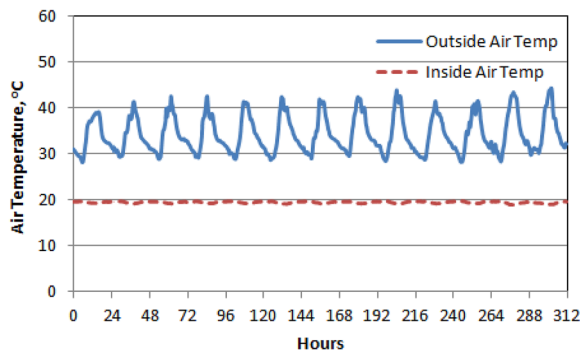


Fig. 14 Variation of internal and external air temperature in the test room during the period of 15 September, 2022 to 27 September, 2022

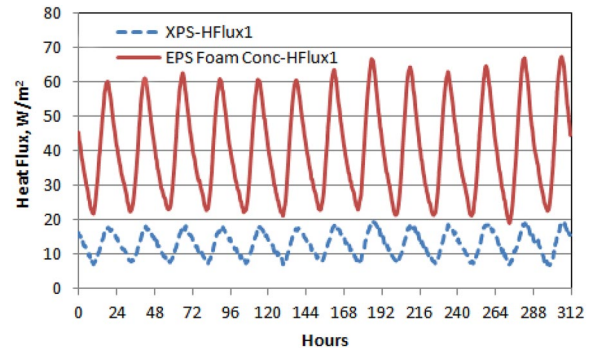


Fig. 16 Heat flow rate variation through the two test systems during the period of 15 September, 2022 to 27 September, 2022

through the sandwiched EPS foam-mortar concrete wall system sample is about three times that through the sandwiched XPS concrete wall system sample, similar to the heat flux results obtained using data set-1. The running average of the thermal resistant (*R*-value) approaches to a fixed value which is presented in Fig. 13.

3.3 Experimental Data Set-3: Testing Period—15 September, 2022 to 27 September, 2022

The experimental data set-3 was collected during 13 days from 15 September, 2022 to 27 September, 2022 at the same location of the two test samples used to obtain data set-1 and set-2. The air temperature measured exterior and interior of the test set-up room is shown in Fig. 14. The average interior air temperature is almost constant at about 19.3 °C, same as that recorded during the acquisition of data sets 1 and 2, and the exterior air temperature fluctuated from 28.2 °C to 44.2 °C, with an average value of 34.3 °C. The average exterior air temperature calculated using data set 3 is about 1.5 °C lower than that calculated using data set 2. The minimum difference of air temperature between the interior and exterior of the test

room is 8.9 °C. Fig. 15 shows the variation of the internal and external surface temperature of the two test samples. Variation of the heat flow rate, calculated using data set-3 is shown in Fig. 16.

The data in Fig. 15 illustrates that the measured surface temperature displays a trend similar to that observed with data set-1 and set-2, i.e., displays cyclic variations. As shown in the results depicted in Fig. 16, the heat flow rate variation is also cyclic for both test samples, with an average value of 12.8 W/m² for the sandwiched XPS concrete wall system sample and 40.7 W/m² for the sandwiched EPS foam-mortar concrete wall system sample. The average heat flux through the sandwiched EPS foam-mortar concrete wall system sample is about three times that through the sandwiched XPS concrete wall system sample, similar to the heat flux results obtained using data set-1 and set-2. The thermal resistance (*R*-value), which converges to a steady value, is plotted in Fig. 17.

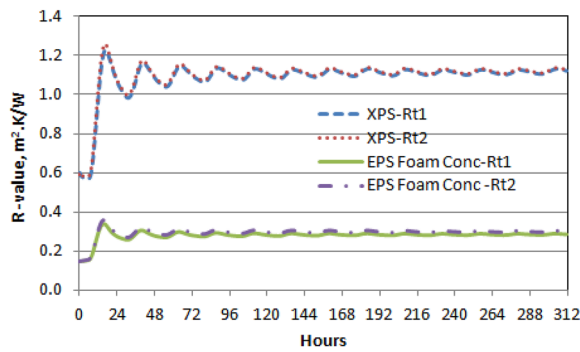


Fig. 17 R-value plot of the two test systems for data set 3

4 Results and Discussion

The thermal performance of the wall panels was analyzed by collecting 3-sets of data. Equations (1, 2 and 3), were utilized to compute the thermal parameters and the results are given in Tables 2, 3, 4, 5, 6 and 7.

The experimental results show that for the sandwiched XPS concrete sample, the U -value is between 0.804 and 0.862 $W/m^2 K$ with an average of 0.837 $W/m^2 K$ and the R -value is between 1.122 and 1.160 $m^2 K/W$ with an average of 1.143 $m^2 K/W$. For the sandwiched EPS foam-mortar concrete wall system sample, the U -value is between 2.362 and 2.733 $W/m^2 K$ with an average of 2.5267 $W/m^2 K$ and the R -value is between 0.275 and 0.299 $m^2 K/W$ with an average of 0.293 $m^2 K/W$. The values of U -value (air to air) at two locations of the two systems of wall panels tested are presented in Table 2. The U -values at the two locations and the three testing periods are not significantly different.

Tables 3 and 4 show that the convergence criterion stipulated by the ASTM-C1155 (ASTM Co 1155, 2021) and ISO-9869-1 (ISO 9869-1, 2014) standards has been met for all experimental results. The R -values after completion of the experiment were compared with the R -values computed at 6, 12 and 24 h before the end of the

Table 2 U -value of the two types of tested wall panel systems

Experimental data set	Test period	Test duration, days	U -value (air to air), $W/m^2 K$			
			Sandwiched XPS concrete		Sandwiched EPS beads foam-mortar concrete	
			Location 1	Location 2	Location 1	Location 2
1	Aug. 16–26	11	0.823	0.804	2.527	2.362
2	Sep. 01–12	12	0.833	0.810	2.587	2.404
3	Sep 15–27	13	0.862	0.842	2.733	2.544

Table 3 R -value of the sandwiched XPS concrete wall panel system

Experimental data set	Test period	Test duration, days	R -value (surface to surface), $m^2 K/W$		Convergence factor: $CR_6, CR_{12}, CR_{24}, \%$	ASTM C1155 and ISO 9869 convergence criteria satisfied (yes/no)
			R -value (surface to surface), $m^2 K/W$			
			Location-1	Location-2		
1	Aug. 16–26	11	1.145	1.151	0.2–0.7	Yes
2	Sep. 01–12	12	1.149	1.160	0.2–0.9	Yes
3	Sep 15–27	13	1.122	1.128	0.4–0.9	Yes

CR_n ($n=6, 12,$ and 24) are the convergence factors at 6, 12, and 24 h before the end of measurements

Table 4 R -value of the sandwiched EPS beads foam-mortar concrete wall panel system

Experimental data set	Test period	Test duration, days	R -value (surface to surface), $m^2 K/W$		Convergence factor: $CR_6, CR_{12}, CR_{24}, \%$	ASTM C1155 and ISO 9869 convergence criteria satisfied (Yes/No)
			R -value (surface to surface), $m^2 K/W$			
			Location-1	Location-2		
1	Aug. 16–26	11	0.275	0.288	0.2–0.9	Yes
2	Sep. 01–12	12	0.280	0.296	0.0–1.2	Yes
3	Sep 15–27	13	0.283	0.299	0.0–1.3	Yes

CR_n ($n=6, 12,$ and 12) are the convergence factors at 6, 12, and 24 h before the end of measurements

Table 5 Thermal performance evaluation results of the sandwiched XPS concrete wall panel system

Experimental data set	Test period	Test duration, days	U-value (air to air), W/m ² K	R-value (surface to surface), m ² K/W	Mean temperature ^a , °C
1	Aug. 16–26	11	0.813	1.148	29.9
2	Sep. 01–12	12	0.822	1.155	30.0
3	Sep 15–27	13	0.852	1.125	29.9
Mean =			0.829	1.142	30.0
Standard deviation =			0.02053	0.01562	–
Coefficient of variation ^b , CV, %			2.48	1.37	–

^a The procedure described in ASTM C1155-21 was used in the calculation of the mean test temperature

^b CV = Standard deviation divided by the average value; and then multiplied by 100

Table 6 Results of the thermal performance evaluation of the sandwiched EPS beads foam-mortar concrete wall panel system

Experimental data set	Test period	Test duration, days	U-value (air to air), W/m ² K	R-value (surface to surface), m ² K/W	Mean temperature ^a , °C
1	Aug. 16–26	11	2.444	0.288	28.4
2	Sep. 01–12	12	2.496	0.296	28.7
3	Sep 15–27	13	2.638	0.291	29.0
Mean =			2.526	0.292	28.7
Standard deviation =			0.10048	0.00412	–
Coefficient of variation ^b , CV, %			3.98	1.41	–

^a The procedure described in ASTM C1155-21 was used in the calculation of the mean test temperature

^b CV = Standard deviation divided by the average value; and then multiplied by 100

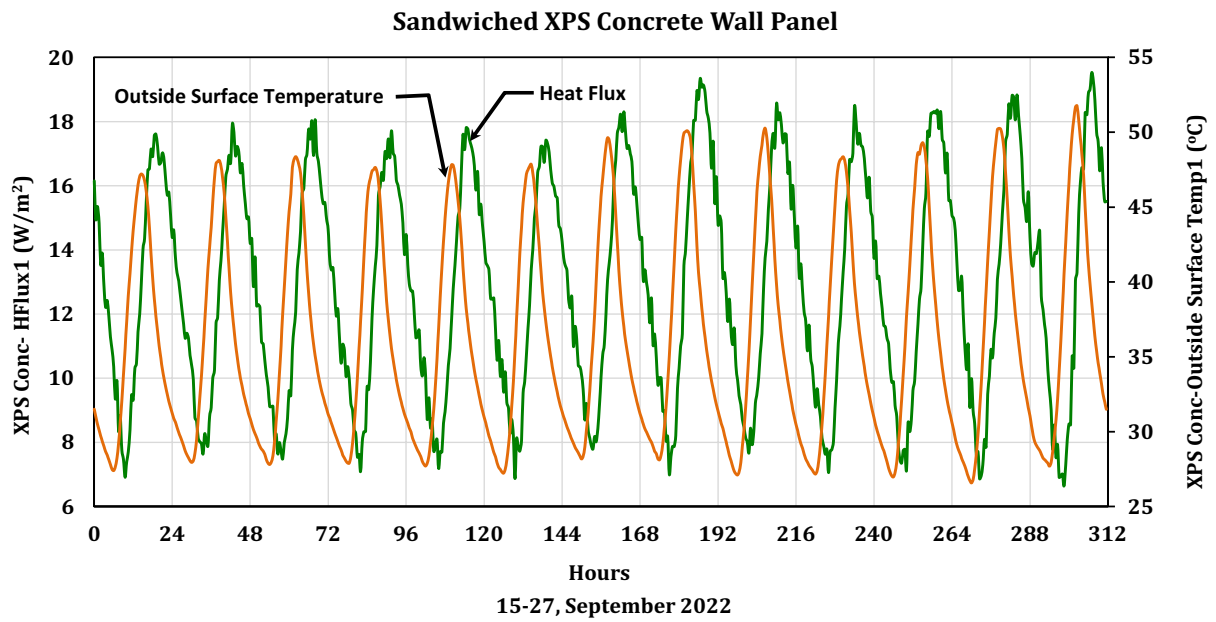
Table 7 Comparison of the thermal parameters of the two types of tested concrete wall panel systems

Panel type	U-value (air to air) W/m ² K	R-value (surface to Surface) m ² K/W	Mean Temp., °C
1. Sandwiched XPS concrete wall panel	0.837	1.143	30.0
2. Sandwiched EPS beads foam-mortar concrete wall panel	2.527	0.293	28.7

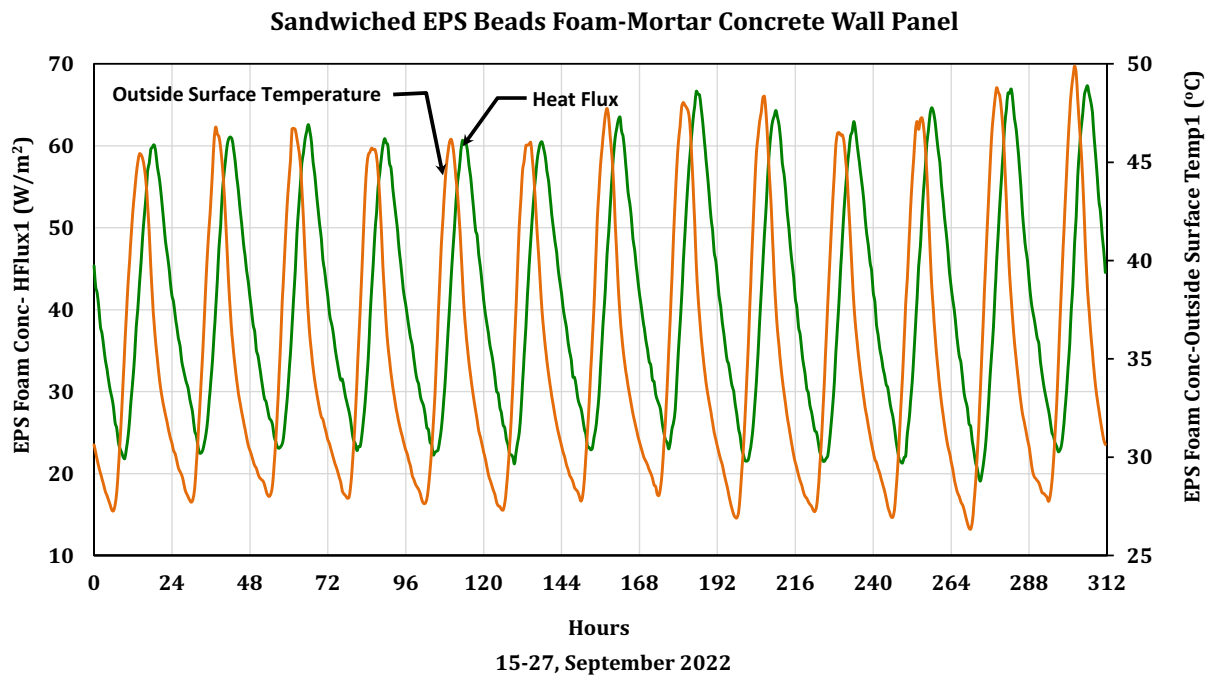
experiment, i.e., $R(t - 6 \text{ h})$, $R(t - 12 \text{ h})$, and $R(t - 24 \text{ h})$. For this purpose, the convergence factor (CR_n) was calculated using Eq. (3) for n values of 6, 12 and 24 h to verify the satisfaction of the criteria specified in the ASTM C1155 (ASTM Co 1155, 2021) standard. The results show that the convergence factor for all n values is much less than 10% and 5% of the R -value at the end of measurement mentioned by ASTM C1155 (ASTM Co 1155, 2021) and by ISO 9869-1 (ISO 9869, 2014) standards, respectively.

Results of the evaluation of the thermal performance of the sandwiched XPS concrete wall system and the

sandwiched EPS foam-mortar concrete wall system wall panel systems are presented in Tables 5 and 6, respectively. The three sets of measured data for both tested samples were analyzed statistically. The standard deviation of the U -values and R -values is between 0.02053 to 0.10048 W/m² K and 0.00412 to 0.01562 m² K/W, respectively. The Coefficient of variation (CV) of the R -value of the sandwiched XPS concrete wall system and sandwiched EPS foam-mortar concrete wall system panels is in the range of 1.37 to 1.41%, which met the ASTM C1155 (ASTM Co 1155, 2021) criterion of being less than 10%. The results of the thermal efficiency evaluation of



(a)



(b)

Fig. 18 Variation of heat flow rate and outside surface temperature for the two test systems during the period of 15 September, 2022 to 27 September, 2022. **a** Sandwiched XPS concrete wall panel. **b** Sandwiched EPS beads foam-mortar concrete wall panel

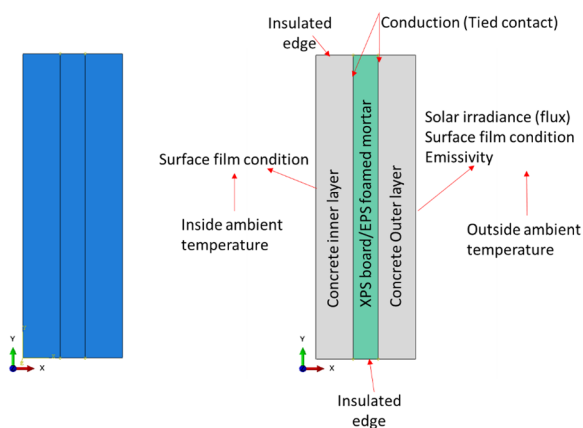


Fig. 19 FEM model scheme

Table 8 Material properties of the panel’s layers used in ABAQUS model

Layer	Density (kg/m ³)	Specific heat (J/kg K)	Thermal conductivity (W/m K)
Outer concrete	2400	920	2.0
Inner concrete	2400	920	2.0
EPS foamed mortar	530	1100	0.25
XPS board	40	1300	0.05

the two different types of tested concrete wall panel samples are displayed in Table 7. It is evident from the results that the *U*-value of the sandwiched EPS foam-mortar concrete wall system sample is more than three times that of the sandwiched XPS concrete wall system sample.

Thus, the thermal performance of the sandwiched XPS concrete wall system panel is much better than that of the sandwiched EPS foam-mortar concrete wall system panel.

The variation of rate of heat flow and external surface temperature of the two test samples is plotted in Fig. 18 to demonstrate the time lag between the maximum heat flow rate on the internal surface and the maximum external surface temperature. Even though the peak temperature on the external surface occurred around 14:00 h, the maximum heat flux was not recorded until about 18:30 h, i.e. a lag of about 4.5 h.

5 FEM Validation Set-1: Testing Period—16 August, 2022 to 26 August, 2022

5.1 FEM Details and Input

For the case of data Set-1, the recorded surface temperature and heat flux of the investigated panels were validated with the simulation based on method of finite elements. The heat transfer through the panels is analyzed using transient heat conditions in the ABAQUS environment. Fig. 19 shows the scheme of the developed 2D-models and Table 8 lists the material properties of the panel’s layers that used as input in the model.

All side edges are assigned as insulated surfaces, the inner surface has a condition of convection boundary, and the outer surface is exposed to solar radiation and convection boundary conditions. The contact between the surfaces of the intermediate layer (XPS/EPS layer) and the outer layers (concrete layers) are assumed to be perfectly bonded. This is modeled in ABAQUS as a Tied Contact element at the desired surfaces which allow for

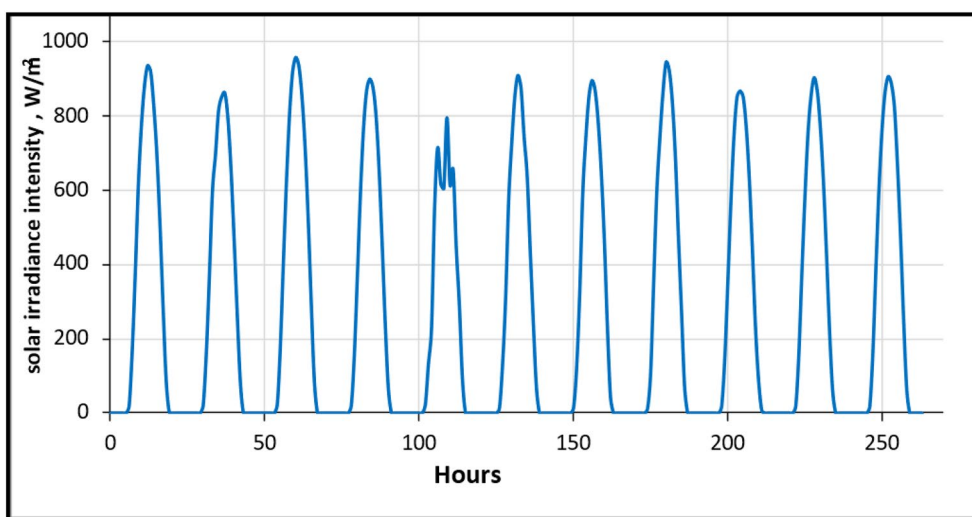
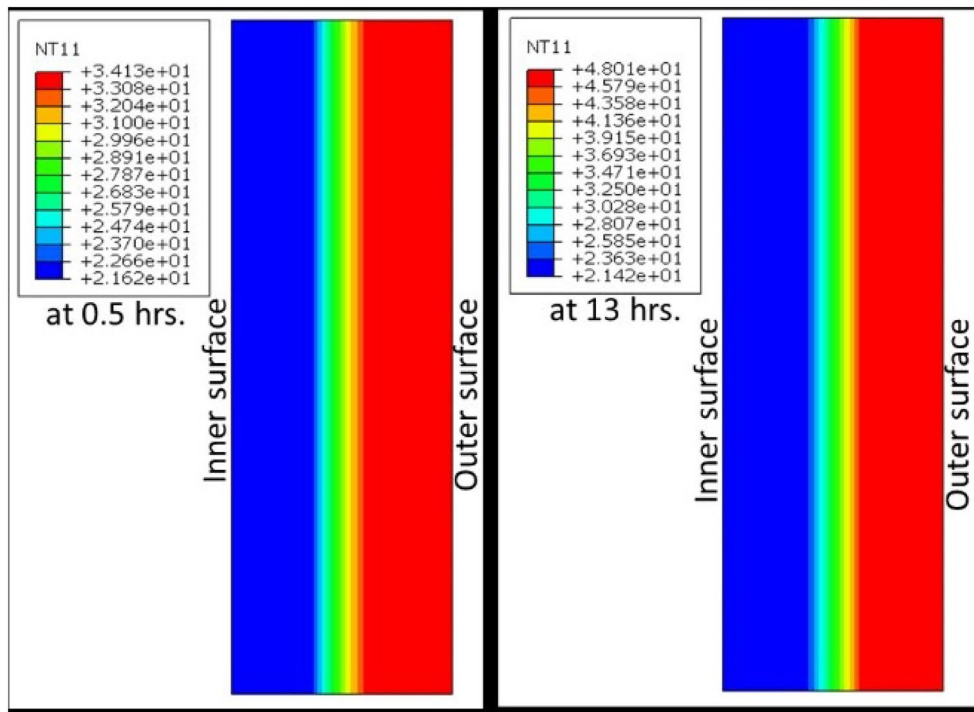
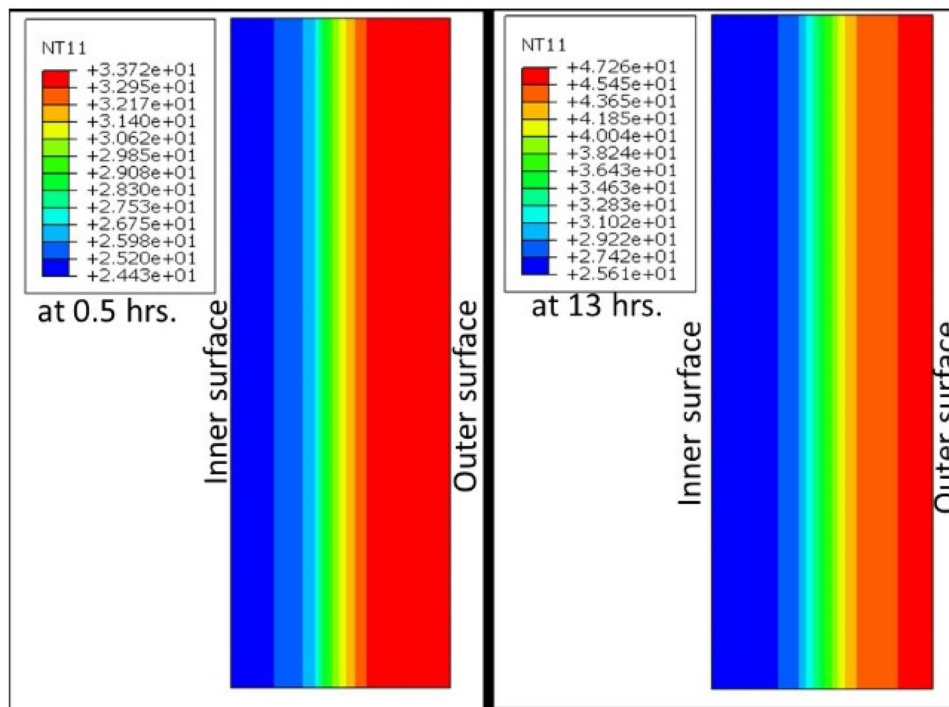


Fig. 20 Solar irradiance intensity during the period of 16 August, 2022 to 26 August, 2022



(a)



(b)

Fig. 21 Temperature profile. **a** Sandwiched XPS concrete wall panel. **b** Sandwiched EPS beads foam-mortar concrete wall panel

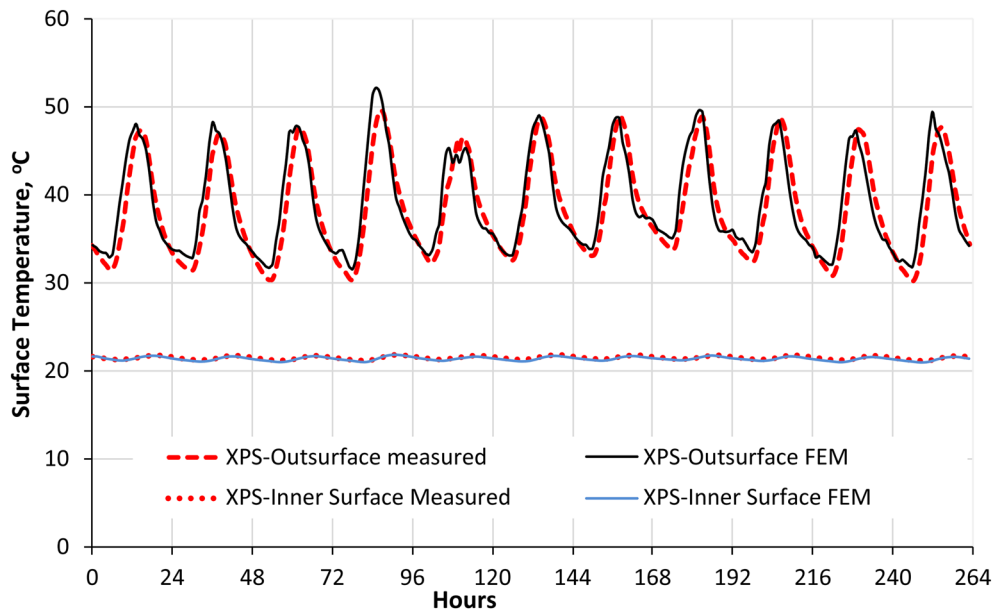


Fig. 22 Comparison of FEM with the measured temperature of the sample with XPS-board during the 16 August, 2022 to 26 August, 2022

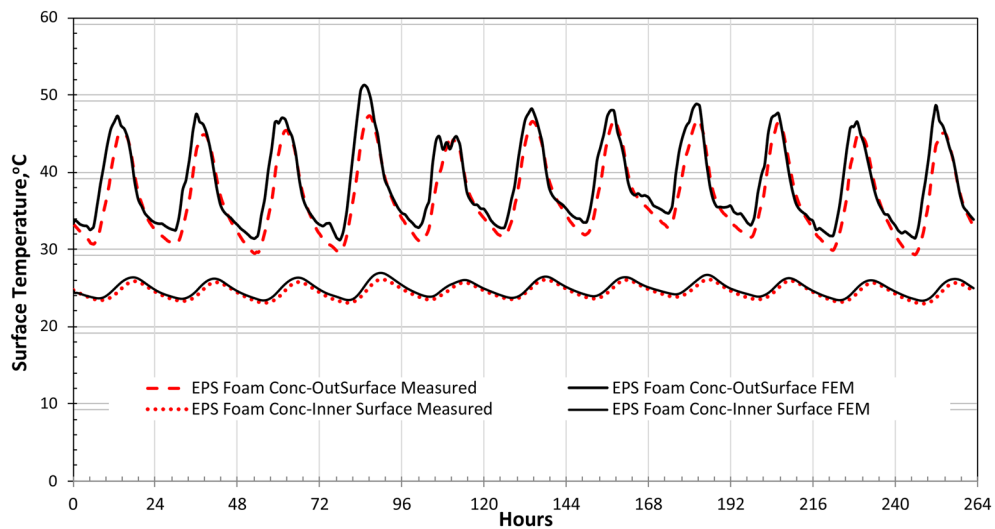


Fig. 23 Comparison of FEM with the measured temperature of the sample with EPS-foamed mortar during the 16 August, 2022 to 26 August, 2022

thermal transmission by conduction. The field measurement of the outside and inside air temperature are input as sink/ambient temperature in the model where the surface film coefficient for the outer and inner surfaces are $65 \text{ W/m}^2\text{K}$ and $8.3 \text{ W/m}^2\text{K}$, respectively. For the case of outer surface, a solar radiation intensity, Fig. 20, is applied as flux with absorption coefficient of 0.6. The model is meshed using heat transfer element type (DC2D4) with fine mesh having a maximum size of 5 mm results in a total of 4880 elements.

5.2 FEM Results

The output of the simulation is compared with the measured data for Set-1 (period 16 August, 2022 to 26 August, 2022) and presented in graphical form. Fig. 21 shows the temperature profile for both panels at the beginning of the recorded data and after 13 h where the temperature reached the first top peak. The hourly temperature change on the outer and inner surfaces is shown in Figs. 22 and 23 with good agreement for both panels with XPS board and EPS foamed mortar, respectively. The

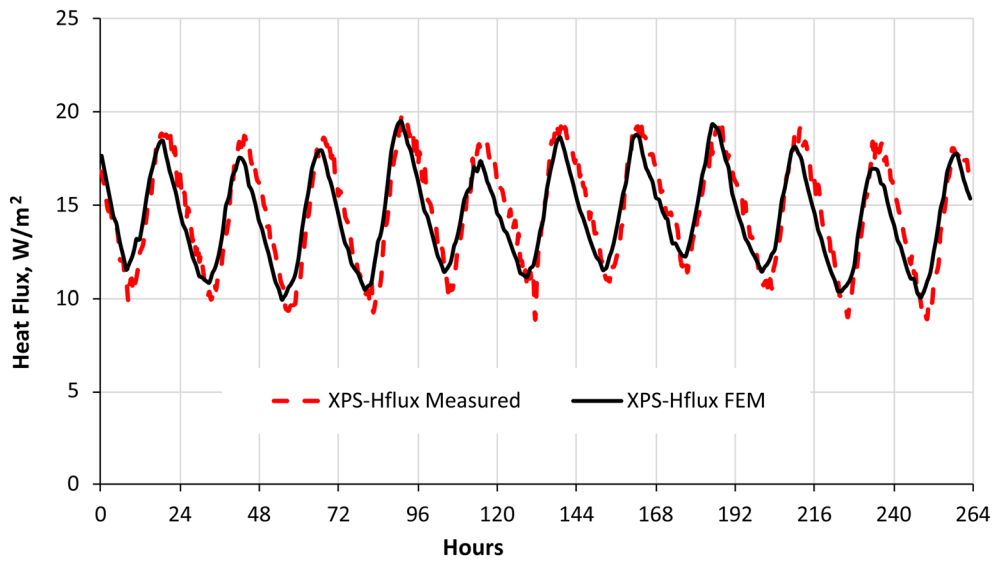


Fig. 24 Comparison of FEM with the measured heat flux of the sample with XPS-board during the 16 August, 2022 to 26 August, 2022

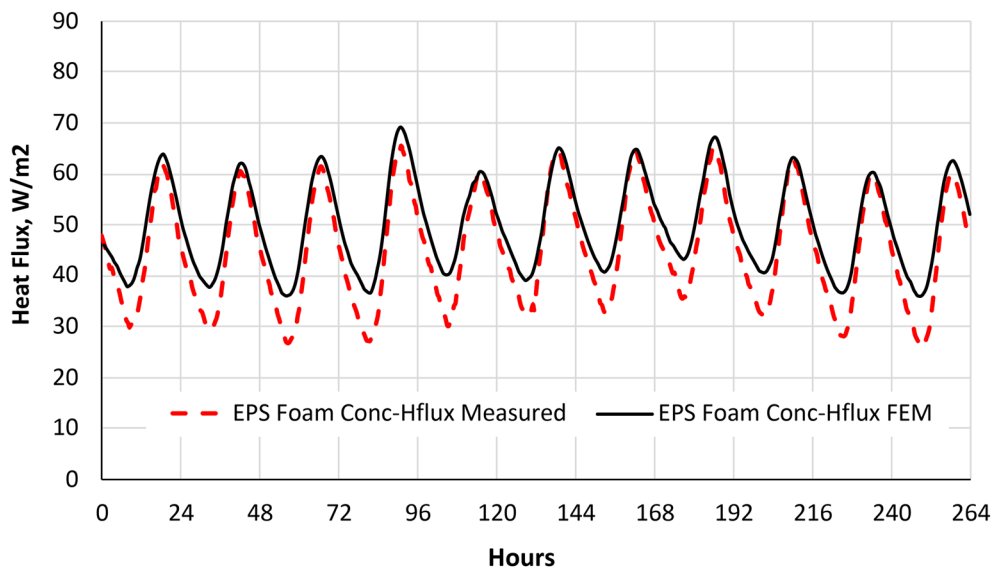


Fig. 25 Comparison of FEM with the measured heat flux of the sample with EPS-foamed mortar during the 16 August, 2022 to 26 August, 2022

simulation can also predict the heat flux through the panels as shown in Figs. 24 and 25 for panels with XPS board and EPS foamed mortar, respectively.

6 Conclusions

Following conclusion was drawn from the analysis of the data obtained from this comparative study of the sandwiched EPS beads foam-mortar concrete sample and sandwiched XPS concrete sample.

1. The maximum intensity of the horizontal global solar irradiance recorded during the measurement period at the test location is 984 W/m². The internal air temperature is almost constant at about 19.3 °C and the external air temperature fluctuated during the monitoring period from 31.2 °C to 47.5 °C with an average value of 37.2 °C.
2. The external surface temperature of the sandwiched XPS concrete wall system panel is higher than that of the sandwiched EPS foam-mortar concrete wall sys-

tem. However, the trend is reversed for the internal surface.

- The U -values (thermal transmittance) for air to air for sandwiched XPS concrete wall system and sandwiched EPS foam-mortar concrete wall system panels were 0.837 and 2.527 W/m²K, respectively. The mean R -values (thermal resistance) for surface to surface for the sandwiched XPS concrete wall system and sandwiched EPS foam-mortar concrete wall system panels were 1.143 and 0.293 m² K/W, respectively.
- The heat flow rate variation is also cyclic for both test samples, with an average value of 14.7 W/m² for sandwiched XPS concrete wall system and 45.2 W/m² for sandwiched EPS foam-mortar concrete wall system. The results also indicate that the average heat flux through the sandwiched EPS foam-mortar concrete wall system panel is about three times that through the sandwiched XPS concrete wall system sample.
- The time lag between the maximum heat flow rate on the internal surface and the maximum external surface temperature is almost the same for the two tested panel systems, which was around 4.5 h.
- The results show that the convergence factor for all n values is much less than 10% and 5% of the R -value at the end of the experiment as mentioned by ASTM C1155 and by ISO 9869-1 standards, respectively indicating that the measurement period used to record each data set is sufficient.
- The results show that the U -value of the sandwiched EPS foam-mortar concrete wall system panel is more than three times that of the sandwiched XPS concrete wall system panel. Thus, the thermal performance of the sandwiched XPS concrete wall system panel is much better than that of the sandwiched EPS foam-mortar concrete wall system panel.
- The output of the simulation by the method of finite element using ABAQUS is compared with the measured data for Set-1 for the period from 16 August, 2022 to 26 August, 2022. The hourly temperature change on the outer and inner surfaces has good agreement for both panels with XPS board and EPS foamed mortar.
- The simulation could also predict the heat flux through the two panels investigated.

Abbreviations

C	Thermal conductance (W m ⁻² K ⁻¹)
CR_n	Convergence factor (%)
CV	Coefficient of variation (%)
d	Wall thickness (m)
q	Heat flow rate (W m ⁻²)
R -value	Thermal resistance (m ² KW ⁻¹)

R_T	Total thermal resistance (m ² KW ⁻¹)
T_e	Exterior air temperature (°C)
T_i	Interior air temperature (°C)
T_{eo}	Exterior surface temperature (°C)
T_{si}	Interior surface temperature (°C)
U -value	Thermal transmittance (W m ⁻² K ⁻¹)
XPS	Extruded polystyrene
EPS	Expanded polystyrene

Subscripts

i	Interior
n	Number of hours
e	Exterior
s	Surface

Index

j	Individual measurements
m	Total number of measurements

Acknowledgements

The support provided by the Research & Innovation of King Fahd University of Petroleum & Minerals, Dhahran, Saudi Arabia is highly acknowledged by the authors.

Author contributions

LMH: Conceptualization, Data curation, Formal analysis, Writing Original draft. AA: Data curation, Formal analysis, Validation, Writing Original draft. MI: Investigation, Validation, Visualization, Writing Original draft, Reviewing and Editing. MRA: Resources, Investigation, Data curation, Formal analysis, Visualization, Reviewing and Editing. MAS: Validation, Visualization, Reviewing and Editing.

Funding

The authors declare that no funds or grants were received during the preparation of this manuscript.

Availability of data and materials

All data generated or analyzed during this study are included in this published article.

Declarations

Ethics approval and consent to participate

Not applicable.

Consent for publication

Not applicable.

Competing interests

The authors have no conflicts of interest to declare that are relevant to the content of this article.

Author details

¹Applied Research Center for Metrology Standards and Testing, Research & Innovation, King Fahd University of Petroleum and Minerals, 31261 Dhahran, Saudi Arabia. ²Department of Civil Engineering, College of Engineering and Information Technology, Onaizah Colleges, Qassim, Saudi Arabia.

Received: 30 November 2023 Accepted: 11 March 2024

Published online: 11 June 2024

References

- Abdelrahman, M. A., Said, S. A. M., & Ahmad, A. (1993). A comparison of energy consumption and cost-effectiveness of four masonry materials in Saudi Arabia. *Energy the International Journal*, 18(11), 1181–1186.
- Ahmad, A., Maselehuddin, M., & Hadhrami, L. M. (2014). In situ measurement of thermal transmittance and thermal resistance of hollow reinforced precast concrete walls. *Energy and Buildings*, 84, 132–141.

- Ahmad, A., & Hadhrami, L. M. (2009). Thermal performance and economic assessment of masonry bricks. *Thermal Science*, 13(4), 221–232.
- Al-Aijlan, S. A. (2006). Measurements of thermal properties of insulation materials by using transient plane source technique. *Journal of Applied Thermal Engineering*, 26, 2184–2191.
- Aldossary, N. A., Rezgui, Y., & Kwan, A. (2014). Domestic energy consumption patterns in a hot and arid climate: A multiple-case study analysis. *Renewable Energy*, 62, 369–378.
- Al-Hadhrami, L. M., & Ahmad, A. (2009). Assessment of thermal performance of different types of masonry bricks used in Saudi Arabia. *Applied Thermal Engineering*, 29, 1123–1130.
- Al-Hammad M., Said, S.A.M., & Washburn, B. (2005). Thermal and economic performance of insulation for hot climates—final report. *King Abdulaziz City for Science and Technology (KACST)*, Research Project AR-8-049, Saudi Arabia
- American Society for Testing and Materials, ASTM Co 1060-11a .(2015). Standard practice for thermographic inspection of insulation installations in envelope cavities of frame buildings. *Annual Book of ASTM Standards*, vol. 04.06. West Conshohocken, PA, USA.
- American Society for Testing and Materials, ASTM Co 1155 .(2021). Standard practice for determining thermal resistance of building envelope components from the in-situ data. *Annual Book of ASTM Standards*, vol. 04.06, West Conshohocken, PA, USA.
- American Society for Testing and Materials, ASTM Co1046 .(2021). "Standard practice for in-situ measurement of heat flux and temperature on building envelope components. *Annual Book of ASTM Standards*, vol. 04.06, West Conshohocken, PA, USA.
- Annual Report. (2016). Annual Statistical Booklet for Electricity and Seawater Desalination Industries. *Electricity and Cogeneration Regulatory Authority*, www.ecra.gov.sa, Riyadh, Kingdom of Saudi Arabia.
- Bagasi, A. A., & Calautit, J. K. (2020). Experimental field study of the integration of passive and evaporative cooling techniques with Mashrabiya in hot climates. *Energy and Buildings*, 225, 110325.
- Biddulph, P., Gori, V., Elwell, C. A., Scott, C., Rye, C., Lowe, R., & Oreszczyn, T. (2014). Inferring the thermal resistance and effective thermal mass of a wall using frequent temperature and heat flux measurements. *Energy and Buildings*, 78, 10–16.
- Budaiwi, A., Abdou, M., & Al-Homoud, M. (2002). Variations of thermal conductivity of insulation materials under different operating temperatures: impact on envelope-induced cooling load. Proc., *First Symposium on Energy Conservation and Management in Buildings*, King Fahd University of Petroleum & Minerals, p. 159–173.
- Cabeza, L. F., Castell, A., Medrano, M., Martorell, I., Perez, G., & Fernandez, I. (2010). Experimental study on the performance of insulation materials in Mediterranean construction. *Energy and Building*, 42, 630–636.
- Courville, G. E., & Beck, J. V. (1989). Techniques for in-situ determination of thermal resistance of lightweight board insulation. *Journal of Heat Transfer*, 111, 274–280.
- Desogus, G., Mura, S., & Ricciu, R. (2011). Comparing different approaches to in-situ measurement of building components thermal resistance. *Energy and Building*, 43, 2613–2620.
- Elhadidy, M.A., Ul-Haq, M., & Ahmad, A. (2001). Electric energy consumption in selected residential buildings at KFUPM, Dhahran, Saudi Arabia. Proc., *Mediterranean Conference for Environment and Solar.*, Beirut, Lebanon, Nov. 16–18, COMPLES 2000, IEEE, Vol. EX493.
- Flanders, S.N. (1985). The convergence criterion in measuring building R-values. *Thermal Performance of the Exterior Envelopes of Buildings*, ASHRAE, Atlanta, GA, pp. 204–209.
- Francesco, A., Francesco, D., Giorgio, B., & Francesco, B. (2014). Evaluating in situ thermal transmittance of green buildings masonries—A case study. *Case Studies in Construction Materials*, 1, 53–59.
- Giorgio, B., Francesco, B., Antonella, R., Danilo, C., Marco, S., Gianluca, V., Francesco, A., & Luca, E. (2018). A model for the improvement of thermal bridges quantitative assessment by infrared thermography. *Applied Energy*, 211, 854–864.
- Gori, V., Marincioni, V., Biddulph, P., & Elwell, C. A. (2017). Inferring the thermal resistance and effective thermal mass distribution of a wall from in-situ measurements to characterize heat transfer at both the interior and exterior surfaces. *Energy and Buildings*, 135, 398–409.
- Guo-liang, A., Ning-jun, D., Ya-zhou, X., & Chao-gang, Q. (2017). Study on the thermal properties of hollow shale blocks as self-insulating wall materials. *Advances in Materials Science and Engineering*, 2017, 12.
- International Standard for Standardization, ISO 9869-1:2014. Thermal insulation-building elements—In-situ measurement of thermal resistance and thermal transmittance-Part 1: Heat flow meter method.
- Iqbal, A., Mubin, S., Gavrişyk, E., Masood, R., Roy, K., & Moradibistouni, M. (2022). A comparative performance analysis of different insulation materials installed in a residential building of a cold region in Pakistan. *Journal of Composites Science*, 6(6), 165. <https://doi.org/10.3390/jcs6060165>
- Kanagaraj, B., Kiran, T., Gunasekaran, J., Nammalvar, A., Arulraj, P., Gurupatham, B. G. A., & Roy, K. (2022). Performance of sustainable insulated wall panels with geopolymer concrete. *Materials*, 15(24), 8801. <https://doi.org/10.3390/ma15248801>
- Kanagaraj, B., Nammalvar, A., Andrushia, A. D., Gurupatham, B. G. A., & Roy, K. (2023). Influence of nano composites on the impact resistance of concrete at elevated temperatures. *Fire*, 6, 135. <https://doi.org/10.3390/fire6040135>
- Li, F. G., Smith, Z. P., Biddulph, P., Hamilton, I. G., Lowe, R., Mavrogianni, A., Oikonomou, E., Raslan, R., Stamp, S. A., Stone, A., et al. (2015). Solid-wall U-values: Heat flux measurements compared with standard assumptions. *Building Research & Information*, 43(2), 238–252.
- Luo, C., Moghtaderi, B., Hands, S., & Page, A. (2011). Determining the thermal capacitance, conductivity and the convective heat transfer coefficient of a brick wall by annually monitored temperatures and total heat fluxes. *Energy and Buildings*, 43, 379–385.
- Peng, C., & Wu, Z. (2008). In-situ measuring and evaluating the thermal resistance of building construction. *Energy and Building*, 40, 2076–2082.
- Roberto, G., Benat, A., & Peru, E. (2017). Experimental thermal performance assessment of a prefabricated external insulation system for building retrofiting. *Environmental Sciences*, 38, 155–161.
- Sassine, E. (2016). A practical method for in-situ thermal characterization of walls—A case studies. *Thermal Engineering*, 8, 84–93.
- Wit de, S., Malkawi, A. M., & Augenbroe, G. (2004). *Advanced building simulation*. New York: Spon Press.

Publisher's Note

Springer Nature remains neutral with regard to jurisdictional claims in published maps and institutional affiliations.

Luai Mohammed Alhems PhD, Director, Applied Research Center for Metrology, Standards and Testing, Research & Innovation, King Fahd University of Petroleum and Minerals, Dhahran-31261, Saudi Arabia.

Aftab Ahmad MS, Research Engineer-III, Applied Research Center for Metrology, Standards and Testing, Research & Innovation, King Fahd University of Petroleum and Minerals, Dhahran-31261, Saudi Arabia.

Mohammed Ibrahim PhD, Research Engineer-III, Applied Research Center for Metrology, Standards and Testing, Research & Innovation, King Fahd University of Petroleum and Minerals, Dhahran-31261, Saudi Arabia.

Mohammed Rizwan Ali MS, Research Engineer-III, Applied Research Center for Metrology, Standards and Testing, Research & Innovation, King Fahd University of Petroleum and Minerals, Dhahran-31261, Saudi Arabia.

Madyan A. Al-Shugaa PhD, Assistant Professor, Department of Civil Engineering, College of Engineering and Information Technology, Onaizah Colleges, Qassim, Saudi Arabia.